Anti-PD-L1 antibodies promote cellular proliferation by activating the PD-L1-AXL signal relay in liver cancer cells

Toshimitsu Tanaka[1,2], Hironori Koga[1,2], Hiroyuki Suzuki[1,2], Hideki Iwamoto[1,2], Takahiko Sakaue[1,2], Atsutaka Masuda[1,2], Toru Nakamura[1,2], Jun Akiba[3], Hirohisa Yano[4], Takuji Torimura[1,2], and Takumi Kawaguchi[1]

[1]Division of Gastroenterology, Department of Medicine, Kurume University School of Medicine
[2]Liver Cancer Research Division, Research Center for Innovative Cancer Therapy, Kurume University
[3]Department of Diagnostic Pathology, Kurume University Hospital
[4]Department of Pathology, Kurume University School of Medicine

Corresponding author
Hironori Koga, M.D., Ph.D.
Professor
Division of Gastroenterology,
Department of Medicine,
Kurume University School of Medicine
67 Asahi-machi, Kurume 830-0011, Japan
Email: hirokoga@med.kurume-u.ac.jp
Tel: +81-942-31-7561
Fax: +81-942-34-2623

Running title: PD-L1-AXL interaction promotes cellular proliferation

Abbreviations: ERK, extracellular signal-regulated kinase; shRNA, small hairpin RNA; Ab, antibody; ICI, Immune checkpoint inhibitor; PD-1, programmed cell death-1; PD-L1, programmed cell death-ligand 1; HPD, hyperprogressive disease; Dur, durvalumab; Atz, atezolizumab; CTL, cytotoxic T lymphocyte; EMT, epithelial-mesenchymal transition; TAM, tumor-associated macrophage; Treg, regulatory T cell; HRP, horseradish peroxidase; qRT, quantitative real-time; KD, knockdown; RT, room temperature; PBS-T, PBS containing 0.05% Tween-20; DAPI, 4',6-diamino-2-phenylindole; p-RTK, phosphorylated receptor tyrosine kinase; TBS, Tris-buffered saline; IP, immunoprecipitation; PNGase, peptide-N-glycosidase; NOD/SCID, NOD/ShiJic-*scid*Jcl; IR, insulin receptor; IGF-1R, insulin-like growth factor-1 receptor; WT, wild-type

PD-L1-expressing cells; 4NQ, unglycosylated PD-L1 mutant cells

Keywords: hyperprogressive disease, tumor microenvironment, immune checkpoint inhibitor, glycosylation, interprotein interaction

Electronic word count: 5,524 (excluding words in References)

Figures: 6

Tables: 1

Supplementary Figures: 2

ABSTRACT

Background Immune checkpoint inhibitors (ICIs) are emerging treatments for advanced hepatocellular carcinoma (HCC); however, evidence has shown they may induce hyperprogressive disease via unexplained mechanisms.

Methods In the current study, we investigated the possible stimulative effect of ICIs on programmed cell death-ligand 1 (PD-L1)-harboring liver cancer cells under immunocompetent cell-free conditions.

Results The sarcomatous HAK-5 cell line displayed the highest expression of PD-L1 among 11 human liver cancer cell lines used in this study. HLF showed moderate expression, while HepG2, Hep3B, and HuH-7 did not show any. Moreover, sarcomatous HCC tissues expressed high levels of PD-L1. We observed approximately 20% increase in cell proliferation in HAK-5 cells treated with anti-PD-L1 antibodies, such as durvalumab and atezolizumab, for 48 h compared with that of those treated with the control IgG and the anti-PD-1 antibody pembrolizumab. No response to durvalumab or atezolizumab was shown in PD-L1-nonexpressing cells. Loss-of-function and gain-of-function experiments for PD-L1 in HAK-5 and HepG2 cells resulted in a significant decrease and increase in cell proliferation, respectively. Phosphorylated receptor tyrosine kinase array and immunoprecipitation revealed direct interactions between PD-L1 and AXL in tumor cells. This was stabilized by extrinsic anti-PD-L1 antibodies in a glycosylated PD-L1-dependent manner. Activation of AXL, triggering signal relay to the Akt and Erk pathways, boosted tumor cell proliferation both *in vitro* and in xenografted tumors in NOD/SCID mice.

Conclusion Collectively, this suggests that anti-PD-L1 antibodies stimulate cell proliferation via stabilization of the PD-L1-AXL complex in specific types of liver cancer, including in HCC with mesenchymal components.

Significance

Therapeutic anti-PD-L1 antibodies promote cell proliferation by stabilizing the PD-L1-AXL complex in PD-L1-abundant neoplasms, including in HCC with mesenchymal components. Such a mechanism may contribute to the development of hyperprogressive disease.

Introduction

The elucidation of immune checkpoint mechanisms has led to major advances in cancer therapy. One of the major targets of antibodies (Abs) against identified immune checkpoint molecules, or immune checkpoint inhibitors (ICIs), is the programmed cell death-1 (PD-1)/programmed cell death-ligand 1 (PD-L1) pathway. PD-1 is mainly found on the cell membrane of cytotoxic T lymphocytes (CTLs), whereas PD-L1 is widely expressed on neoplastic and non-neoplastic cells, including on dendritic and monocytic cells. The binding of PD-L1 to PD-1 leads to CTL apoptosis, resulting in a state of immune exhaustion (1-3). ICIs can improve CTL function and induce antitumor effects by blocking the PD-1/PD-L1 signaling pathway (4). The PD-1/PD-L1 pathway regulates various cellular biological effects other than cancer immune evasion mechanisms, such as cell proliferation (5), epithelial-mesenchymal transition (EMT) (6), stemness (7), and glucose metabolism (8, 9). However, most of the detailed mechanisms remain unclear.

Hyperprogressive disease (HPD), a condition wherein tumors grow rapidly after treatment with ICIs, has recently been observed in ICI-treated patients (10). In primary liver cancer, the incidence of HPD was reported as 10% in ICI monotherapy-treated patients with the disease (11). Thus far, two underlying mechanisms of HPD have been proposed. One is that the Fc region of the anti-PD-1 antibody (Ab) differentiates local tumor macrophages into M2-like tumor-associated macrophages (TAMs), tilting the tumor microenvironment toward an immunosuppressive state (12). The other is that administered anti-PD-1 Abs activate PD-1$^+$ regulatory T cells (Tregs) and suppress anti-tumor immunity (13-15). However, the precise mechanism of HPD remains unclear. A previous report (5) suggests that anti-PD-L1 Abs may activate proliferative signals in liver cancer cells via its target molecule PD-L1 and induce HPD. In this study, we investigated whether anti-PD-L1 Abs directly interact with PD-L1 and stimulate the proliferation of liver cancer cells under immunocompetent cell-free conditions.

Materials and Methods

Patients and tumor tissues

Thirty-three patients (26 male and 7 female) with HCC participated in this study (Table 1). The patients underwent curative resection of HCCs between 2000 and 2017 at Kurume University Hospital. Informed consent for this study was obtained from all patients according to the principles stated in the Declaration of Helsinki. The study plan was approved by the Ethical Committee of Kurume University (study registration no. 16264). HCC was diagnosed by at least two pathologists (J.A. and H.Y.), independently according to the WHO classification. Histological grades of the 33 HCCs were as follows: 5 well-differentiated, 5 moderately differentiated, 5 poorly differentiated, and 18 sarcomatous types. HCC tissues of the three patients treated with

trans-catheter arterial chemoembolization (TACE) showed sarcomatous features.

Immunohistochemistry and staining scores

Five-μm thick tumor tissue sections were prepared from paraffin-embedded blocks and boiled for 30 min in a high-pH target retrieval solution (Agilent Technologies, Inc., Santa Clara, CA, USA). Sections were pre-blocked with normal horse serum and incubated with an anti-PD-L1 Ab (clone E1L3N; Cell Signaling Technology, Inc., Danvers, MA, USA) for human samples and with an anti-Ki-67 Ab (clone MIB1 (Dako); Agilent Technologies, Inc.) for mouse samples at 4°C overnight. Positive immunoreactive signals were visualized using the EnVision+ system (Dako) and a DAB kit (Dako). Hematoxylin and rabbit IgG were used for nuclear counterstaining and negative controls, respectively.

PD-L1 staining scores were evaluated semiquantitatively according to the previous report (16) for the intensity of positive signals and stain-positive area. For the Ki-67 labeling index, Ki-67-positive cells/1000 tumor cells examined were automatically counted after setting the threshold for binarization in the ImageJ 1.53 software. For immunohistochemical assessment of infiltrative cells in mouse xenografted tumors including $CD3^+$ cells, $CD8^+$ cells, dendritic cells, macrophages, and natural killer (NK) cells, the primary Abs anti-CD3-ε Ab, anti-CD8-α Ab, anti-CD11c Ab, anti-F4/80 Ab, and anti-NK1.1 Ab (all obtained from Cell Signaling Technology) were used, respectively. All images of the stained sections were obtained with an all-in-one fluorescence microscope (BZ-X700, KEYENCE, Osaka, Japan).

Cell lines

Liver cancer cell lines HepG2, HuH-7, and Hep3B were purchased from the American Type Culture Collection (Manassas, VA, USA). HLF was obtained from the Japanese Cancer Research Resources Bank (Tokyo, Japan). HAK-5 was originally established from peritoneal effusion in a patient with sarcomatous HCC in the Department of Pathology of Kurume University School of Medicine (17). All cell lines were grown and passaged under conditions reported previously (16).

ICIs and IgGs

The ICIs including pembrolizumab, durvalumab, and atezolizumab were purchased from Selleck (Houston, TX, USA). IgGs was from Medical and Biological Laboratories Co, Ltd (Tokyo, Japan).

Western blotting

Cell- and tissue-derived protein preparation and SDS-PAGE were performed as in our previous study (16). Abs for the following molecules were obtained from Cell Signaling

Technology: PD-L1, PD-L2, PD-1, p-AXL, AXL, p-Akt, Akt, phosphorylated extracellular signal-regulated kinase (p-Erk)1/2, and total Erk1/2: all were used at 1:1,000 in dilution. Abs against GAPDH and TurboGFP were purchased from Santa Cruz Biotechnology, Inc. (Santa Cruz, CA, USA) and OriGene Technologies, Inc. (Rockville, MD, USA), respectively. To visualize protein-derived signals, horseradish peroxidase (HRP)-labeled secondary Abs, ECL Plus Western Blotting Detection Reagents (Amersham Pharmacia Biotech, Buckinghamshire, UK), and an image analyzer (LAS-4000; Fujifilm, Tokyo, Japan) equipped with Multi Gauge software, version 3.0 (Fujifilm) were used (16).

Quantitative real-time (qRT)-PCR analysis

TaqMan-based qRT-PCR assay was carried out using a 7500 Fast Real Time PCR System (Applied Biosystems, Foster City, CA, USA) according to the previous report (16). The pre-designed probes were PD-L1 (CD274) (Assay ID, Hs00204257_m1) and AXL (Hs01064444_m1). Gene expression levels relative to those of GAPDH (Hs02758991_g1) were calculated by the ΔΔ-CT method implemented in StepOne Software 2.0 (Applied Biosystems).

Overexpression of PD-L1

A green fluorescent protein (GFP)-tagged PD-L1-expressing plasmid (RC213071) and an empty vector (PS100010) were purchased from OriGene Technologies. To establish stably transfected clones, HuH-7 and HepG2 cells were transfected with PD-L1 cDNA or the mock vector using TransIT-LT1 (Mirus, Madison, WI, USA). After transfection, PD-L1-overexpressing clones (PD-L1-HuH-7 and PD-L1-HepG2) were selected with 400 μg/mL G418 (Nacalai Tesque). Control cell clones (Ctrl-HuH-7 and Ctrl-HepG2) were selected in a similar manner.

Knockdown (KD) of PD-L1 and ectopic expression of PD-L1 mutants

Lentiviral transduction particles containing PD-L1 shRNAs (sc-39699) or non-targeting shRNAs (sc-108080) were obtained from Santa Cruz Biotechnology. Stable PD-L1-KD cells and mock cells were selected using 1 μg/mL puromycin (Sigma-Aldrich by Merck KGaA, Darmstadt, Germany) according to our previous study (16).

To generate wild-type PD-L1-expressing and unglycosylated PD-L1 mutant (4NQ) cells (7), we obtained pGIPz-PD-L1 WT and pGIPz-PD-L1 4NQ plasmids, respectively, from Addgene (Watertown, MA, USA), and then packaged them into lentiviruses (VectorBuilder Inc., Chicago, IL, USA). The viral constructs were designed to silence endogenous PD-L1 expression by shRNA and enforce the expression of exogenous wild-type or unglycosylated PD-L1 (7). Cells were transfected with the viral particles using TransIT-Lenti Transfection Reagent (Mirus) and the stable clones were selected using 1 μg/mL puromycin.

Cell proliferation assay

To assess cell proliferation, a CDA-1000 automated cell counter (Sysmex, Kobe, Japan) was used for counting the viable cells in suspension on days 0, 2, 4, and 6. To evaluate the proliferation-stimulating role of anti-PD-L1 Abs in PD-L1-expressing liver cancer cells, durvalumab (25 ng/mL) and atezolizumab (25 ng/mL) were used in comparison with the control IgG isotype (25 ng/mL) and the anti-PD-1 Ab pembrolizumab (25 ng/mL), and the cell number was counted on day 2. To ensure the function of AXL, the specific agonist growth arrest specific 6 (Gas6) (R&D systems, Inc., Minneapolis, MN, USA) and the specific inhibitor bemcentinib (Selleck) were used.

Immunocytochemistry

For immunocytochemical staining, cells were fixed with fresh 4% paraformaldehyde at 25 ± 2°C for 15 min and washed in PBS containing 0.05% Tween-20 (PBS-T). Blocking of nonspecific reactions and incubation with primary and secondary Abs were performed as described previously (18). For nuclear staining, VECTASHIELD Mounting Medium with 4’,6-diamino-2-phenylindole (DAPI) (Burlingame, CA, USA) was used. For double staining of PD-L1 and AXL, a mouse monoclonal anti-PD-L1 Ab and a rabbit monoclonal anti-AXL Ab (both, Cell Signaling Technology, Inc.) were used as primary Abs and Alexa Fluor 488 goat anti-mouse IgG (H+L) Ab and Alexa Fluor 568 goat anti-rabbit IgG (H+L) Ab (both, Molecular Probes, Eugene, OR, USA) were used as secondary Abs. Samples incubated with rabbit and/or mouse IgG were utilized as negative controls. Immunofluorescent signals were visualized with a BZ-X700 microscope (KEYENCE).

p-Receptor Tyrosine Kinase (p-RTK) array

HAK-5 cells were treated with atezolizumab (25 ng/mL) or IgG isotype (25ng/mL) for 24 h. The harvested cell-derived lysates were subjected to a comparative analysis of p-RTK protein levels using a Proteome Profiler Human Phospho-RTK Array Kit (R&D Systems, Minneapolis, MN, USA). The p-RTK array membranes were pre-blocked with 5% bovine serum albumin-containing 0.01 M Tris-buffered saline (TBS) (pH 7.4) for 1 h and then incubated with cell lysates containing equal amounts of protein between test and control samples. After washing with TBS containing 0.1% Tween-20, the membranes were incubated with an HRP-marked anti-phosphotyrosine Ab for 2 h at 25±2 °C. Visualization of target proteins and their densitometric analysis were performed in a similar manner to that of the Western blotting section.

Immunoprecipitation (IP)

Total cell lysates prepared with an NP-40-based lysis buffer were incubated with Abs against

PD-L1 and AXL followed by Recombinant Protein G Agarose (Thermo Fisher Scientific, Waltham, MA, USA) at 4 °C. Antigen-Ab-bead complexes were centrifuged and washed with Tris-based buffer. Immunoblots were probed with Abs to PD-L1, p-AXL, AXL, and ubiquitin (A5) (Santa Cruz Biotechnology) and detected as in the Western blotting section.

Deglycosylation by peptide-N-glycosidase (PNGase) F

Total cell lysates were incubated with PNGase F (N-Zyme Scientifics, Doylestown, PA, USA) at 37 °C for 1 h to digest *N*-linked oligosaccharides. Both glycosylated and unglycosylated PD-L1 proteins were then detected by Western blotting.

Xenograft mouse model

PD-L1-HepG2 and Ctrl-HepG2 cells (5.0×10^6) were subcutaneously implanted into the flank of 5-week-old male NOD/ShiJic-*scid*Jcl (NOD/SCID) mice (Clea Japan, Inc., Osaka, Japan). When the measured tumor volume ($0.52 \times \text{length} \times \text{width}^2$) reached 150 mm^3, the tumor-bearing mice were randomly divided into four treatment groups (n=6 in each) as follows: 1) Ctrl-HepG2-injected mice treated with IgG, 2) Ctrl-HepG2-injected mice treated with atezolizumab, 3) PD-L1-HepG2-injected mice treated with IgG, and 4) PD-L1-HepG2-injected mice treated with atezolizumab. IgG and atezolizumab were intraperitoneally administered three times a week at the dose of 10 mg/kg/mouse. The tumor volumes were measured every two days. Mice were sacrificed four weeks after the beginning of the treatments, and the tumors were resected for subsequent immunohistochemistry and Western blotting. All animal experiments were ethically performed according to the guidelines described previously (16).

Statistical analysis

Data analyses were performed using JMP Pro 15.0 software (JMP, Tokyo, Japan). An unpaired Student's t-test was used to assess statistically significant differences between the two groups. All data are expressed as the mean ± SEM.

RESULTS

Expression of PD-L1 in human HCC tissues and liver cancer cell lines

Immunohistochemically, membranous PD-L1 was clearly expressed in poorly differentiated HCC tissues, weakly expressed in moderately differentiated tissues, and faintly or not expressed in well-differentiated tissues (Fig. 1A). Sarcomatous HCC, followed by poorly-differentiated HCC, significantly expressed the highest levels of PD-L1 out of the 33 HCCs studied (Fig. 1B). Western blot analysis using liver cancer cell lines showed that PD-L1 was consistently and markedly expressed in HAK-5, a sarcomatous HCC cell line (17). PD-L1 was also shown to be moderately

expressed in HLF, with the appearance of mesenchymal cell features, although it was not expressed in HepG2, Hep3B, or HuH-7 (Fig. 1C). Neither PD-L2 nor PD-1 expression was faint or absent in all the tested cell lines (Fig. 1C). The expression trend of PD-L1 was also confirmed at the transcriptional level (Fig. 1D).

Gene silencing of PD-L1 in the HAK-5 cell line

KD of PD-L1 with shRNAs in HAK5 cells was confirmed by Western blotting and qRT-PCR (Figs. 2A and B). Significantly decreased cell proliferation was demonstrated in PD-L1-KD HAK-5 cells compared with the control mock cells (Fig. 2C), suggesting a direct involvement of PD-L1 in promoting tumor cell proliferation.

Anti-PD-L1 Abs drive tumor cell proliferation

To prove the accelerating potential of PD-L1 in tumor cell proliferation, we stimulated HCC cells with anti-PD-L1 Abs. When HAK-5 cells were exposed to the anti-PD-L1 Ab atezolizumab, cell proliferation was significantly increased compared with cells in the IgG-treated group (Fig. 3A), and the increase was dosage-dependent up to 25 ng/mL (Fig. 3B). Durvalumab, another PD-L1 Ab, also promoted cell proliferation (approximately 20%) like atezolizumab, but the anti-PD-1 Ab pembrolizumab and IgG did not in 48-h incubation (Fig. 3C).

Gain-of-function experiments using PD-L1/GFP-overexpressing liver cancer cells

We generated PD-L1/GFP-overexpressing liver cancer cell lines based on the commonly used liver cancer cells HepG2 and HuH-7 (Figs. 4A and B). Immunocytochemically, the ectopic expression of PD-L1/GFP was localized on the plasma membrane in HepG2 cells, in contrast to the cytoplasm in HuH-7 cells (Fig. 4C). Interestingly, HepG2 cells, but not HuH-7 cells, sharply responded to atezolizumab treatment and proliferated in a dosage-dependent manner (Fig. 4D). Given that PD-L1 is a type I transmembrane protein (19), its physiological localization is suggested to be crucial for intracellular signaling of PD-L1-mediated cell proliferation.

AXL complexes with PD-L1

Since the localization of PD-L1 on the cell membrane was critical for anti-PD-L1 Ab-promoted cell proliferation, we explored potential collaborating membranous molecules, including RTKs. Comprehensive array analysis of p-RTKs in the atezolizumab-treated HAK-5 cells revealed that insulin receptor (IR), insulin-like growth factor-1 receptor (IGF-1R), and AXL were phosphorylated in comparison with the IgG-treated cells (Fig. 5A). Then, we evaluated the expression levels of the most activated molecule, AXL, by qRT-PCR and Western blotting; however, there was no upregulation found from either analysis (Fig. 5B). Considering possible inter-molecular interactions between PD-L1 and AXL, we performed IP-Western blot experiments, and found that the two molecules were complexed together during treatment with anti-PD-L1 antibodies (Figs. 5C and D). Colocalization of the two molecules PD-L1 and AXL, suggesting a strong inter-molecular interaction, was visualized by immunocytochemistry in the atezolizumab-treated HAK-5 cells (Fig. 5E). To confirm that the simultaneous use of an AXL inhibitor and an anti-PD-L1

antibody has clinical relevance in the treatment of HCC, the following two experiments were performed: one is to ascertain the cell-proliferating function of the Gas6-stimulated AXL, and the other is to assess the inhibiting effect of the specific AXL inhibitor bemcentinib on the boosted cell proliferation by anti-PD-L1 antibodies plus Gas6 in PD-L1-expressing HCC cells. As a result, Gas6 significantly promoted cell proliferation of the PD-L1-expressing HAK-5 cells under co-stimulation with anti-PD-L1 antibodies, suggesting that the AXL signaling was boosted (Supplementary Fig. 1A). In the inhibition experiment, bemcentinib canceled the boosted proliferation of the cells treated with both anti-PD-L1 antibody and Gas6 (Supplementary Fig. 1B).

N-glycosylation is necessary for the binding of PD-L1 with AXL

Glycosylation of proteins plays an important role in protein-protein interactions. Thus, we speculated that highly glycosylated PD-L1, displaying N-glycosylation at four conserved asparagine residues, greatly contributes to forming the PD-L1/AXL complex. In an IP-Western blotting experiment using PNGase F to remove N-glycans from protein substrates of HAK-5 cells, the thick band representing glycosylated PD-L1, including 43-kDa bands, completely disappeared following enzymatic treatment, and the PD-L1/AXL interaction was lost accordingly (Fig. 5F). In the next experiment, using the wild-type PD-L1-expressing cells (WT) and unglycosylated PD-L1 mutant cells (4NQ), the binding of PD-L1 to AXL was abolished in unglycosylated 4NQ cells following treatment with atezolizumab (Figs. 5G and H). This implies that direct binding between PD-L1 and AXL is critically dependent on the N-glycosylation of PD-L1.

PD-L1 Abs promotes xenografted tumor growth of PD-L1-overexpressing HepG2 cells

We assessed whether the anti-PD-L1 Ab atezolizumab promotes the growth of xenografted tumors in NOD/SCID mice (Fig. 6A). Since the sarcomatous HAK-5 cells and their mutants (PD-L1-KD HAK-5 cells and the control mock cells) did not form any tumors in the mice, PD-L1-HepG2 and Ctrl-HepG2 cells were used in our animal experiments. Consistent with our *in-vitro* data, the rate of growth of PD-L1-HepG2-based tumors was remarkably accelerated by atezolizumab administration on day 14, followed by a gradual but significant increase in PD-L1-HepG2-based tumors without treatment (Fig. 6A). Growth of Ctrl-HepG2-based tumors, which consisted of cells lacking endogenous PD-L1 expression (Figs. 1C and D), was not promoted by atezolizumab treatment.

Immunohistochemical analysis of Ki-67 showed that atezolizumab-treated PD-L1-HepG2-based tumor tissues displayed the highest index by a significant amount, followed by their untreated counterparts (Fig. 6B). In Western blot analysis for the xenografted tumor tissues was focused on identifying the expressions of AXL and its downstream signaling molecules, including p-Akt, Akt, p-Erk1/2, and Erk1/2. We found that the expressions of p-Akt and p-Erk1/2 were significantly increased in the atezolizumab-treated PD-L1-HepG2-based tumors compared with their untreated counterparts and Ctrl-HepG2-based tumors (Fig. 6C). Our findings indicate that the downstream signal relays of AXL are activated by atezolizumab treatment *in vivo*. Further analysis of infiltrative cells in the xenografted tumors, no significant difference in positive

cells/microscopic field was observed in dendritic cells, macrophages, or NK cells among the four groups (Supplementary Fig. 2). There were no $CD3^+$ cells or $CD8^+$ cells in the tumors (data not shown).

DISCUSSION

In this study, we found that anti-PD-L1 Abs 1) stabilized PD-L1 on the cell surface of liver cancer cells, 2) enhanced the interaction between PD-L1 and AXL in a PD-L1 glycan-dependent manner, and 3) promoted the activation of Akt and Erk1/2, which are downstream signals of AXL, thereby enhancing the proliferation of liver cancer cells, particularly of the sarcomatous type.

First, we found that the expression levels of PD-L1 in human HCC tissues were enhanced in association with the dedifferentiation of the tumor. This was consistent with the previous findings that PD-L1 is strongly expressed in aggressive HCCs with poor prognoses (20). In addition, we found for the first time that PD-L1 expression was strongest in sarcomatous HCC, both *in vitro* and *in vivo*. This finding is supported by the high expression of the protein in sarcomatoid lung carcinoma (21). Therefore, it is thought that the EMT-involved transformation of cancer cells into sarcomatous cells promotes immune evasion by expressing PD-L1 in those cells (6).

It has been suggested that one of the mechanisms of HPD is the activation and numerical superiority of $PD\text{-}1^+$ Treg cells in the tumor microenvironment (13, 14). In addition, we hypothesized that direct stimulation of PD-L1-expressing tumors with anti-PD-L1 Abs could be involved in rapid growth during HPD. To prove this hypothesis, we used a simple cell culture without the presence of immunocompetent cells such as dendritic cells and lymphocytes, and found that anti-PD-L1 Abs directly stimulated tumor cell proliferation not only in sarcomatous liver cancer cells that strongly express PD-L1 but also in the cells that ectopically overexpress PD-L1. At this point, it is noteworthy that the proliferation-promoting effect of anti-PD-L1 Abs was observed only when the overexpressed PD-L1 was localized on the plasma membrane of the tumor cells. Recently, it has been shown that PD-L1 expressed on the cell membrane can be translocated to the nucleus by deacetylation of lysine residues in the cytoplasmic domain (22) and that the activated genes through its nuclear translocation were those regulating immune response and inflammation, but not cellular proliferation. This is consistent with previous findings that the PD-L1 molecule does not have any specific domain structure for stimulating cellular proliferation. These findings together led us to speculate that PD-L1 may be involved in transmitting cell-proliferating signals into the cancer cells by being conjugated with another molecule localized at the cell membrane. We hypothesized that membrane-localized molecules such as RTKs that are professionally involved in cell proliferation may be involved in this and therefore conducted a p-RTK array experiment. Thus, we identified AXL as a partner of PD-L1 in promoting tumor cell proliferation in the presence of anti-PD-L1 Abs. AXL is isolated from human

chronic myelogenous leukemia (23), and its expression is correlated with tumor malignancy and poor prognosis of patients with various cancers (24). In HCC, AXL has been reported to be involved in the suppression of apoptosis and the enhancement of cell proliferation and migration (25), and its expression level correlates with tumor recurrence rate and poor prognosis of patients (26).

Glycans that interact with proteins *in vivo* often exist in clusters of multiple glycans (27). Therefore, we investigated the role of glycosylation of PD-L1 molecules in the protein-protein interaction between PD-L1 and AXL (28). In general, N-glycosylation (asparagine-linked glycosylation) plays a pivotal role in many biochemical events, including protein-protein interactions (29, 30). In the extracellular domain of PD-L1, four N-glycosylation sites (N35, N192, N200, and N219) have been identified and reported to be required for binding to PD-1 in mediating its immunosuppressive effects (31). Based on these findings, we established a sarcomatous liver cancer cell line, in which intrinsic PD-L1 was silenced and non-glycosylated PD-L1 was overexpressed. The results showed that the PD-L1-AXL interaction was not observed in the cells lacking PD-L1 N-glycosylation. Thus, we revealed, for the first time, such unique interaction between PD-L1 and the oncogene product AXL on the tumor cell membrane in the presence of anti-PD-L1 Abs in a PD-L1 glycan-dependent manner. Interestingly, it was reported that PD-L1 and AXL are co-expressed in renal cell carcinoma with poor prognosis (32). This suggests that the PD-L1-AXL axis is involved in the malignant traits of tumor cells. Furthermore, activation of the PI3K/Akt and/or Erk pathways downstream of AXL is also considered a possible mechanism of PD-L1 upregulation (33). Therefore, our findings indicate that AXL-triggered upregulation of PD-L1 possibly forms a positive feedback loop that stabilizes AXL on the tumor cell membrane and activates downstream signaling of AXL under specific conditions, including in the presence of anti-PD-L1 Abs. Further studies are needed to clarify the clinical relevance of this.

The effects of extrinsic anti-PD-L1 Abs in boosting tumor growth were reproduced in xenografted tumor models of NOD/SCID mice, resulting in the activation of the Akt and Erk pathways. The unique role of the PD-L1-AXL axis in immunodeficient environments does not explain the complicated molecular mechanism of HPD in the human body, but the PD-L1-AXL interaction-mediated enhancement of tumor cell proliferation may occur in patients with the following cancer milieu, in particular: 1) cancers with high expression of PD-L1 and AXL, which undergo EMT-mediated sarcoma-like changes (34), and 2) cancers in the older individuals and patients with a low neutrophil-to-lymphocyte ratio and impaired immune function (35, 36). Very recently, the phase III COSMIC-312 clinical trial, in which atezolizumab was combined with cabozantinib, a multi-kinase inhibitor with anti-AXL activity, displayed the superior efficacy of combination pharmacological therapy in advanced HCCs compared with sorafenib alone (37). As

a result, the median progression-free survival of the combination therapy (6.8 months) was significantly longer than that of sorafenib (4.2 months) (P=0.0012) (37). The outcome suggests that combinatorial usage of AXL inhibitor and anti-PD-L1 Ab may suppress the tumor cell-proliferating role of the Ab in the tumor microenvironment of HCC. The potential of AXL in canceling the anti-PD-L1-induced boost of cell proliferation in sarcomatous HCC cells may support the idea.

In conclusion, this study revealed that anti-PD-L1 Ab stabilizes the PD-L1-AXL complex on the surface of HCC cells and activates the downstream signaling of AXL (*i.e.* the Akt and Erk pathways), thereby boosting tumor cell proliferation. Further analysis of tumor factors, including EMT, sarcomatous changes, and immune checkpoint molecules, as well as patient background, is needed to determine the extent to which the PD-L1-AXL axis impacts the mechanism of HPD.

ACKNOWLEDGEMENTS

We thank Yasuko Imamura and Masako Hayakawa for their technical assistance.

DECLARATIONS

Ethics approval: This study was approved by the Institutional Review Board of Kurume University (study registration no. 16264), and all related procedures conformed to the Declaration of Helsinki.

Funding Support: This work was supported by JSPS KAKENHI (Grant no. 19K17507).

Conflict of interest: The authors disclose no conflicts.

Informed consent:

Informed consent was obtained from all patients according to the principles stated in the Declaration of Helsinki.

Authors' contributions: TTanaka and HK participated in the study conception and design, acquisition of data, interpretation of data, and drafting of the manuscript. AJ and HY provided tissue samples with pathological information and the HAK-5 cell line. HS, HI, TS, AM, and TN participated in the analysis and interpretation of data. TTorimura and TK participated in a critical discussion.

REFERENCES

1) Ishida Y, Agata Y, Shibahara K, Honjo T. Induced expression of PD-1, a novel member of the immunoglobulin gene superfamily, upon programmed cell death. EMBO J 1992;11:3887-3895.

2) Iwai Y, Ishida M, Tanaka Y, Okazaki T, Honjo T, Minato N. Involvement of PD-L1 on tumor cells in the escape from host immune system and tumor immunotherapy by PD-L1 blockade. Proc Natl Acad Sci USA 2002;99:12293-12297.

3) Freeman GJ, Long AJ, Iwai Y, Bourque K, Chernova T, Nishimura H, Fitz LJ, Malenkovich N, Okazaki T, Byrne MC, Horton HF, Fouser L, Carter L, Ling V, Bowman MR, Carreno BM, Collins M, Wood CR, Honjo T. Engagement of the PD-1 immunoinhibitory receptor by a novel B7 family member leads to negative regulation of lymphocyte activation. J Exp Med 2000;192:1027-1034.

4) Kraehenbuehl L, Weng CH, Eghbali S, Wolchok JD, Merghoub T. Enhancing immunotherapy in cancer by targeting emerging immunomodulatory pathways. Nat Rev Clin Oncol 2022;19:37-50.

5) Qiu XY, Hu DX, Chen WQ, Chen RQ, Qian SR, Li CY, Li YJ, Xiong XX, Liu D, Pan F, Yu SB, Chen XQ. PD-L1 confers glioblastoma multiforme malignancy via Ras binding and T Ras/Erk/EMT activation. Biochimica et Biophysica Acta (BBA) - Molecular Basis of Disease 2018;1864:1754-1769.

6) Chen L, Gibbons DL, Goswami S, Cortez MA, Ahn YH, Byers LA, Zhang X, Yi X, Dwyer D, Lin W, Diao L, Wang J, Roybal J, Patel M, Ungewiss C, Peng D, Antonia S, Mediavilla-Varela M, Robertson G, Suraokar M, Welsh JW, Erez B, Wistuba II, Chen L, Peng D, Wang S, Ullrich SE, Heymach JV, Kurie JM, Qin FX. Metastasis is regulated via microRNA-200/ZEB1 axis control of tumour cell PD-L1 expression and intratumoral immunosuppression. Nat Commun 2014;5:5241.

7) Hsu JM, Xia W, Hsu YH, Chan LC, Yu WH, Cha JH, Chen CT, Liao HW, Kuo CW, Khoo KH, Hsu JL, Li CW, Lim SO, Chang SS, Chen YC, Ren GX, Hung MC. STT3-dependent PD-L1 accumulation on cancer stem cells promotes immune evasion. Nat Commun 2018;9:1908.

8) Kim S, Jang JY, Koh J, Kwon D, Kim YA, Paeng JC, Ock CY, Keam B, Kim M, Kim TM, Heo DS, Chung DH, Jeon YK. Programmed cell death ligand-1-mediated enhancement of hexokinase 2 expression is inversely related to T-cell effector gene expression in non-small-cell lung cancer. J Exp Clin Cancer Res 2019;38:462.

9) Ma P, Xing M, Han L, Gan S, Ma J, Wu F, Huang Y, Chen Y, Tian W, An C, Sun H, Sun L. High PD-L1 expression drives glycolysis via an Akt/mTOR/HIF-1α axis in acute myeloid leukemia. Oncol Rep 2020;43:999-1009.

10) Champiat S, Dercle L, Ammari S, Massard C, Hollebecque A, Postel-Vinay S, Chaput N, Eggermont A, Marabelle A, Soria JC, Ferté C. Hyperprogressive disease Is a new pattern of progression in cancer patients treated by anti-PD-1/PD-L1. Clin Cancer Res 2017;23:1920-1928.

11) Xiao LS, Li Q-M, Hu C-Y, Cui H, Hong C, Huang C-Y, Li R-N, Dong Z-Y, Zhu H-B, Liu L. Lung metastasis and lymph node metastasis are risk factors for hyperprogressive disease in primary liver cancer patients treated with immune checkpoint inhibitors. Ann Palliat Med 2021;10:11244-11254.

12) Lo Russo G, Moro M, Sommariva M, Cancila V, Boeri M, Centonze G, Ferro S, Ganzinelli M, Gasparini P, Huber V, Milione M, Porcu L, Proto C, Pruneri G, Signorelli D, Sangaletti S, Sfondrini L, Storti C, Tassi E, Bardelli A, Marsoni S, Torri V, Tripodo C, Colombo MP, Anichini A, Rivoltini L, Balsari A, Sozzi G, Garassino MC. Antibody-Fc/FcR interaction on macrophages as a mechanism for hyperprogressive disease in non-small cell lung cancer subsequent to PD-1/PD-L1 blockade. Clin Cancer Res 2019;25:989-999.

13) Kumagai S, Togashi Y, Kamada T, Sugiyama E, Nishinakamura H, Takeuchi Y, Vitaly K, Itahashi K, Maeda Y, Matsui S, Shibahara T, Yamashita Y, Irie T, Tsuge A, Fukuoka S, Kawazoe A, Udagawa H, Kirita K, Aokage K, Ishii G, Kuwata T, Nakama K, Kawazu M, Ueno T, Yamazaki N, Goto K, Tsuboi M, Mano H, Doi T, Shitara K, Nishikawa H. The PD-1 expression balance between effector and regulatory T cells predicts the clinical efficacy of PD-1 blockade therapies. Nat Immunol 2020;21:1346-1358.

14) Kamada T, Togashi Y, Tay C, Ha D, Sasaki A, Nakamura Y, Sato E, Fukuoka S, Tada Y, Tanaka A, Morikawa H, Kawazoe A, Kinoshita T, Shitara K, Sakaguchi S, Nishikawa H. PD-1+ regulatory T cells amplified by PD-1 blockade promote hyperprogression of cancer. Proc Natl Acad Sci USA 2019;116:9999-10008.

15) Granito A, Muratori L, Lalanne C, Quarneti C, Ferri S, Guidi M, Lenzi M, Muratori P. Hepatocellular carcinoma in viral and autoimmune liver diseases: Role of CD4+ CD25+ Foxp3+ regulatory T cells in the immune microenvironment. World J Gastroenterol 2021;27:2994-3009.

16) Ikezono Y, Koga H, Akiba J, Abe M, Yoshida T, Wada F, Nakamura T, Iwamoto H, Masuda A, Sakaue T, Yano H, Tsuruta O, Torimura T. Pancreatic neuroendocrine tumors and EMT behavior are driven by the CSC marker DCLK1. Mol Cancer Res 2017;15:744-752.

17) Yano H, Ogasawara S, Momosaki S, Akiba J, Kojiro S, Fukahori S, Ishizaki H, Kuratomi K, Basaki Y, Oie S, Kuwano M, Kojiro M. Growth inhibitory effects of pegylated IFN alpha-2b on human liver cancer cells in vitro and in vivo. Liver Int 2006;26:964-975.

18) Koga H, Sakisaka S, Harada M, Takagi T, Hanada S, Taniguchi E, Kawaguchi T, Sasatomi K, Kimura R, Hashimoto O, Ueno T, Yano H, Kojiro M, Sata M. Involvement of p21(WAF1/Cip1), p27(Kip1), and p18(INK4c) in troglitazone-induced cell-cycle arrest in human hepatoma cell lines. Hepatology 2001;33:1087-97.

19) Zhou S, Zhu J, Xu J, Gu B, Zhao Q, Luo C, Gao Z, Chin YE, Cheng X. Anti-tumour potential of PD-L1/PD-1 post-translational modifications. Immunology. 2022 Dec;167(4):471-481.

20) Gao Q, Wang XY, Qiu SJ, Yamato I, Sho M, Nakajima Y, Zhou J, Li BZ, Shi YH, Xiao YS, Xu Y, Fan J. Overexpression of PD-L1 significantly associates with tumor aggressiveness and postoperative recurrence in human hepatocellular carcinoma. Clin Cancer Res 2009;15:971-979.

21) Velcheti V, Rimm DL, Schalper KA. Sarcomatoid lung carcinomas show high levels of programmed death ligand-1 (PD-L1). J Thorac Oncol 2013;8:803-805.

22) Gao Y, Nihira NT, Bu X, Chu C, Zhang J, Kolodziejczyk A, Fan Y, Chan NT, Ma L, Liu J, Wang D, Dai X, Liu H, Ono M, Nakanishi A, Inuzuka H, North BJ, Huang YH, Sharma S, Geng Y, Xu W, Liu XS, Li L, Miki Y, Sicinski P, Freeman GJ, Wei W. Acetylation-dependent regulation of PD-L1 nuclear translocation dictates the efficacy of anti-PD-1 immunotherapy. Nat Cell Biol 2020;22:1064-1075.

23) O'Bryan JP, Frye RA, Cogswell PC, Neubauer A, Kitch B, Prokop C, Espinosa R 3rd, Le Beau MM, Earp HS, Liu ET. Axl, a transforming gene isolated from primary human myeloid leukemia cells, encodes a novel receptor tyrosine kinase. Mol Cell Biol 1991;11:5016-5031.

24) Linger RM, Keating AK, Earp HS, Graham DK. TAM receptor tyrosine kinases: biologic functions, signaling, and potential therapeutic targeting in human cancer. Adv Cancer Res 2008;100:35-83.

25) Reichl P, Dengler M, van Zijl F, Huber H, Führlinger G, Reichel C, Sieghart W,

Peck-Radosavljevic M, Grubinger M, Mikulits W. Axl activates autocrine transforming growth factor-β signaling in hepatocellular carcinoma. Hepatology 2015;61:930-941.

26) Haider C, Hnat J, Wagner R, Huber H, Timelthaler G, Grubinger M, Coulouarn C, Schreiner W, Schlangen K, Sieghart W, Peck-Radosavljevic M, Mikulits W. Transforming growth factor-β and Axl Induce CXCL5 and neutrophil recruitment in hepatocellular carcinoma. Hepatology 2019;69:222-236.

27) Mammen M, Choi SK, Whitesides GM. Polyvalent interactions in biological systems: implications for design and use of multivalent ligands and inhibitors. Angew Chem Int Ed Engl 1998;37:2754-2794.

28) Li CW, Lim SO, Chung EM, Kim YS, Park AH, Yao J, Cha JH, Xia W, Chan LC, Kim T, Chang SS, Lee HH, Chou CK, Liu YL, Yeh HC, Perillo EP, Dunn AK, Kuo CW, Khoo KH, Hsu JL, Wu Y, Hsu JM, Yamaguchi H, Huang TH, Sahin AA, Hortobagyi GN, Yoo SS, Hung MC. Eradication of triple-negative breast cancer cells by targeting glycosylated PD-L1. Cancer Cell 2018;33:187-201.e10.

29) Cheung JC, Reithmeier RA. Scanning N-glycosylation mutagenesis of membrane proteins. Methods 2007;41:451-9.

30) Lopez-Sambrooks C, Shrimal S, Khodier C, Flaherty DP, Rinis N, Charest JC, Gao N, Zhao P, Wells L, Lewis TA, Lehrman MA, Gilmore R, Golden JE, Contessa JN. Oligosaccharyltransferase inhibition induces senescence in RTK-driven tumor cells. Nat Chem Biol 2016;12:1023-1030.

31) Li CW, Lim SO, Xia W, Lee HH, Chan LC, Kuo CW, Khoo KH, Chang SS, Cha JH, Kim T, Hsu JL, Wu Y, Hsu JM, Yamaguchi H, Ding Q, Wang Y, Yao J, Lee CC, Wu HJ, Sahin AA, Allison JP, Yu D, Hortobagyi GN, Hung MC. Glycosylation and stabilization of programmed death ligand-1 suppresses T-cell activity. Nat Commun 2016;7:12632.

32) Terry S, Dalban C, Rioux-Leclercq N, Adam J, Meylan M, Buart S, Bougoüin A, Lespagnol A, Dugay F, Moreno IC, Lacroix G, Lorens JB, Gausdal G, Fridman WH, Mami-Chouaib F, Chaput N, Beuselinck B, Chabaud S, Barros-Monteiro J, Vano Y, Escudier B, Sautès-Fridman C, Albiges L, Chouaib S. Association of AXL and PD-L1 expression with clinical outcomes in patients with advanced renal cell carcinoma treated with PD-1 blockade. Clin Cancer Res 2021;27:6749-6760.

33) Hahn AW, George DJ, Agarwal N. An evolving role for AXL in metastatic renal cell carcinoma. Clin Cancer Res 2021;27:6619-6621.

34) Assi T, Mir O. Hyperprogressive disease in leiomyosarcoma: a threat to the use of single-agent anti-PD-(L)1 therapy? Immunotherapy. 2022;14:271-274.

35) Kanjanapan Y, Day D, Wang L, Al-Sawaihey H, Abbas E, Namini A, Siu LL, Hansen A, Razak AA, Spreafico A, Leighl N, Joshua AM, Butler MO, Hogg D, Chappell MA, Soultani L, Chow K, Boujos S, Bedard PL. Hyperprogressive disease in early-phase immunotherapy trials: clinical predictors and association with immune-related toxicities. Cancer 2019;125:1341-1349.

36) Kim CG, Kim C, Yoon SE, Kim KH, Choi SJ, Kang B, Kim HR, Park SH, Shin EC, Kim YY, Kim DJ, Chung HC, Chon HJ, Choi HJ, Lim HY. Hyperprogressive disease during PD-1 blockade in patients with advanced hepatocellular carcinoma. J Hepatol 2021;74:350-359.

37) Kelley RK, Rimassa L, Cheng AL, Kaseb A, Qin S, Zhu AX, Chan SL, Melkadze T, Sukeepaisarnjaroen W, Breder V, Verset G, Gane E, Borbath I, Rangel JDG, Ryoo BY, Makharadze T, Merle P, Benzaghou F, Banerjee K, Hazra S, Fawcett J, Yau T. Cabozantinib plus atezolizumab versus sorafenib for advanced hepatocellular carcinoma (COSMIC-312): a multicentre, open-label, randomised, phase 3 trial. Lancet Oncol 2022;23:995-1008.

38) Granito A, Forgione A, Marinelli S, Renzulli M, Ielasi L, Sansone V, Benevento F, Piscaglia F, Tovoli F. Experience with regorafenib in the treatment of hepatocellular carcinoma. Therap Adv Gastroenterol 2021;14:17562848211016959.

FIGURE LEGENDS

Figure 1.

Expression of PD-L1 in human HCC tissues and liver cancer cell lines. **A,** PD-L1 is most highly expressed in sarcomatous (Src) HCC tissues, followed by poorly (Por) and moderately (Mod) differentiated HCC tissues. **B,** Immunostaining scores showing Src tissues as having the highest expression of PD-L1. CH, chronic hepatitis. LC, liver cirrhosis. **C and D,** Western blotting and qRT-PCR for PD-L1 expression in human liver cancer cell lines. The sarcomatous HAK-5 cells show the strongest PD-L1 expression at both the protein (**C**) and mRNA (**D**) levels. **, P<0.01 and ***, P<0.001.

Figure 2.

Knockdown (KD) of PD-L1 in the HAK-5 cell line. HAK-5 cells were transfected with PD-L1-targeting shRNAs or control (Ctrl) shRNAs, and their stable transfectants were selected, respectively. **A,** Western blot analysis of the indicated proteins in PD-L1-KD cells and Ctrl mock cells. **B,** *PD-L1* mRNA expression levels quantified by qRT-PCR. **C,** Comparison of cell proliferation between PD-L1-KD cells (red line) and Ctrl mock cells (black line). **, P<0.01.

Figure 3.

Anti-PD-L1 Abs increase tumor cell proliferation. **A,** Cell proliferation under the treatment with atezolizumab (Atz) (25, 50, and 500 ng/mL), 25 ng/mL of IgG, and the vehicle in HAK-5 cells. A significant increase in Atz-treated cell number was observed. *, P<0.05. **B,** Cell number on day 2 following treatment with various concentrations of Atz (5, 10, 25, 50, and 500 ng/mL), 25 ng/mL of IgG, and the vehicle in HAK-5 cells. A significant increase is seen at concentrations of more than or equal to 25 ng/mL of Atz. *, P<0.05. **C,** Comparison of HAK-5 cell number on day 2 following treatment with an anti-PD-1 antibody (25 ng/mL of pembrolizumab (Pem)) and anti-PD-L1 antibodies (25 ng/mL of durvalumab (Dur) and 25 ng/mL of Atz). A significant increase is seen in cells treated with Dur and Atz. IgG, 25 ng/mL. *, P<0.05. **D,** Comparison of the proliferation-promoting activity of Atz (25 ng/mL) on day 2 among the three cell lines HepG2, HuH-7, and HLF. A significant increase in cell proliferation is seen only in Atz-treated HLF cells, which moderately express PD-L1 (See Fig. 1C and D). *, P<0.05.

Figure 4.

Gain-of-function experiment using PD-L1/GFP-overexpressing liver cancer cells. **A,** Immunocytochemistry for PD-L1 (red), counterstained with DAPI for nuclei (blue). Co-localization of GFP (green) and PD-L1 (red) in the PD-L1/GFP-HuH-7 cells (left panels) and PD-L1/GFP-HepG2 cells (right panels) is shown (original magnification x 400). Forced expression

of PD-L1 is localized on the plasma membrane of HepG2 cells, while it is seen in the cytoplasm of HuH-7 cells. **B** and **C,** Overexpression of GFP-tagged PD-L1 in HuH-7 and HepG2 cells (PD-L1/GFP-HuH7 cells and PD-L1/GFP-HepG2 cells) shown by qRT-PCR (**B**) and Western blot analysis (**C**). **D,** Relative cell number on day 2 in PD-L1/GFP-HuH-7 cells (left panel) and PD-L1/GFP-HepG2 cells (right panel) following treatment with 10 and 25 ng/mL of Atz, and 25 ng/mL of IgG. *, P<0.05 and **, P<0.01.

Figure 5.

AXL is a partner molecule of PD-L1, driving cell proliferation. **A,** (Left panel) RTK array analysis exploring RTKs responsible for the Atz-promoted cell proliferation in HAK-5 cells. Atz, 25 ng/mL. IgG, 25 ng/mL. (Right panel) Comparative quantification of spot pixel densities for phosphorylated (p-) RTKs between IgG-treated cells (black columns) and Atz-treated cells (red columns). IR, insulin receptor. IGF-IR, insulin-like growth factor-1 receptor. **B** and **C,** qRT-PCR for evaluating the expression levels of AXL mRNA (**B**) and Western blot analysis (**C**) for evaluating the expressions of AXL and PD-L1 in HAK-5 cells treated with Dur or Atz (both 25 ng/mL). **D,** IP-Western blotting using anti-AXL Ab and anti-PD-L1 Abs to demonstrate AXL-PD-L1 interaction. **E,** Immunocytochemical double staining of PD-L1 and AXL in the Atz-treated HAK-5 cells (upper 4 panels). The lower 4 panels are negative controls. **F,** HAK-5 cells were treated with Atz or IgG (both 25 ng/mL), and the cell lysates were incubated in the presence or absence of PNGase F. Then, the lysates were subjected to IP using anti-AXL Ab, followed by immunoblotting using Abs for AXL and PD-L1. The enzymatic digestion of protein glycosylation leads to the loss of the PD-L1-AXL interaction. **G,** Genetically engineered-unglycosylated PD-L1 mutant cells (4NQ) show no thick bands for glycosylation in PD-L1 compared with the wild-type PD-L1-expressing cells (WT) under treatment with Atz (25 ng/mL). **H,** In Atz-treated 4NQ cells, there is no interaction between PD-L1 and AXL in the IP experiment.

Figure 6.

Atz promotes xenografted tumor growth of PD-L1-overexpressing HepG2 cells in NOD/SCID mice. **A,** Growth of PD-L1-HepG2-based tumors is markedly driven by Atz treatment on day 14, followed by a gradual but significant increase in PD-L1-HepG2-based tumors without treatment. Growth of Ctrl-HepG2-based tumors, consisting of cells lacking endogenous PD-L1 expression, is not promoted by treatment. *, P<0.05; **, P<0.01; and ***, P<0.001. Red asterisks indicate “PD-L1-HepG2 Atz” vs. “PD-L1-HepG2 IgG”, and blue ones “PD-L1-HepG2 IgG” vs. “Ctrl-HepG2 Atz”/“Ctrl-HepG2 IgG”. **B,** Ki-67 staining for representative xenografted tumor tissues (upper panel) and its labeling index (lower panel). The Atz-treated PD-L1-HepG2-based tumors have the significantly highest indices among the 4 groups, followed by the untreated PD-L1-HepG2-based

tumors. *, P<0.05 and **, P<0.01. **C,** Western blot analysis for the expressions of AXL and its downstream signaling molecules, including p-AKT, AKT, p-Erk1/2, and Erk1/2 (left panel). The expression levels of p-AKT and p-Erk1/2 are significantly elevated in the Atz-treated PD-L1-HepG2-based tumors compared with their untreated counterparts and Ctrl-HepG2-based tumors (right panels). *, P<0.05 and **, P<0.01.

Supplementary Figure 1.

AXL stimulated with anti-PD-L1 antibody is more powerful. **A,** Gas6 (200 ng mL), an agonistic ligand for AXL, significantly promotes cell proliferation of the PD-L1-expressing HAK-5 cells under co-stimulation with anti-PD-L1 antibodies. **B,** The boosted cell proliferation is canceled by the specific AXL inhibitor bemcentinib at the concentration of 500 nM, that is IC50 in the cells. Concentrations of IgG, durvalumab (Dur), and atezolizumab (Atz) are all 25 ng/mL. *, P<0.05 and **, P<0.01.

Supplementary Figure 2.

Immunohistochemical analysis of immune cells infiltrated in the xenografted tumors. No significant difference in positive cell numbers or areas/high-power field is shown in dendritic cells ($CD11c^+$), macrophages ($F4/80^+$), or NK cells($NK1.1^+$) among the four groups.

Figure 1

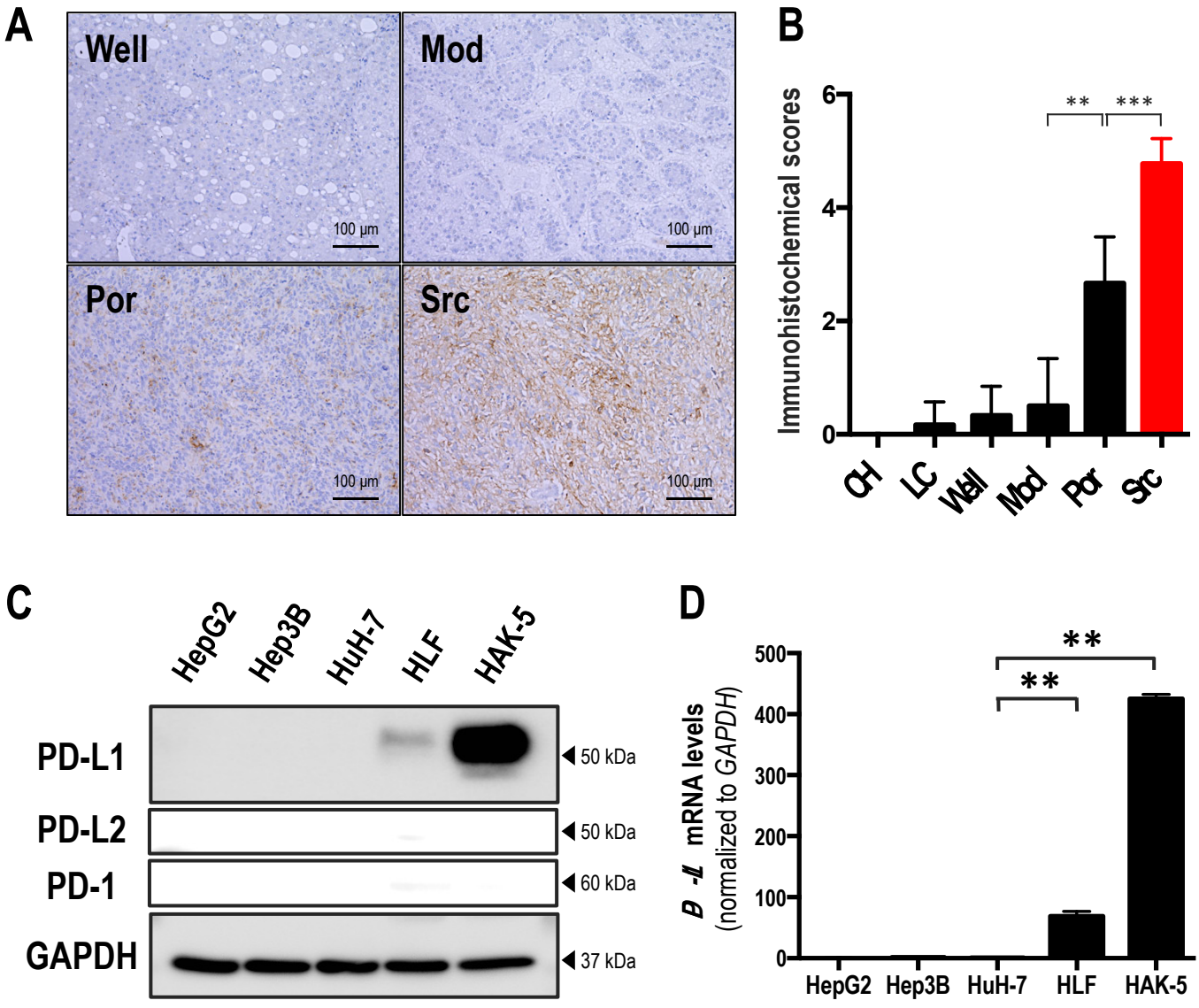
A
Well
Mod
Por
Src
100 μm
B
Immunohistochemical scores
**
***
CH
LC
Well
Mod
Por
Src
C
HepG2
Hep3B
HuH-7
HLF
HAK-5
PD-L1
PD-L2
PD-1
GAPDH
50 kDa
50 kDa
60 kDa
37 kDa
D
PD-L1 mRNA levels
(normalized to GAPDH)
HepG2
Hep3B
HuH-7
HLF
HAK-5

Figure 2

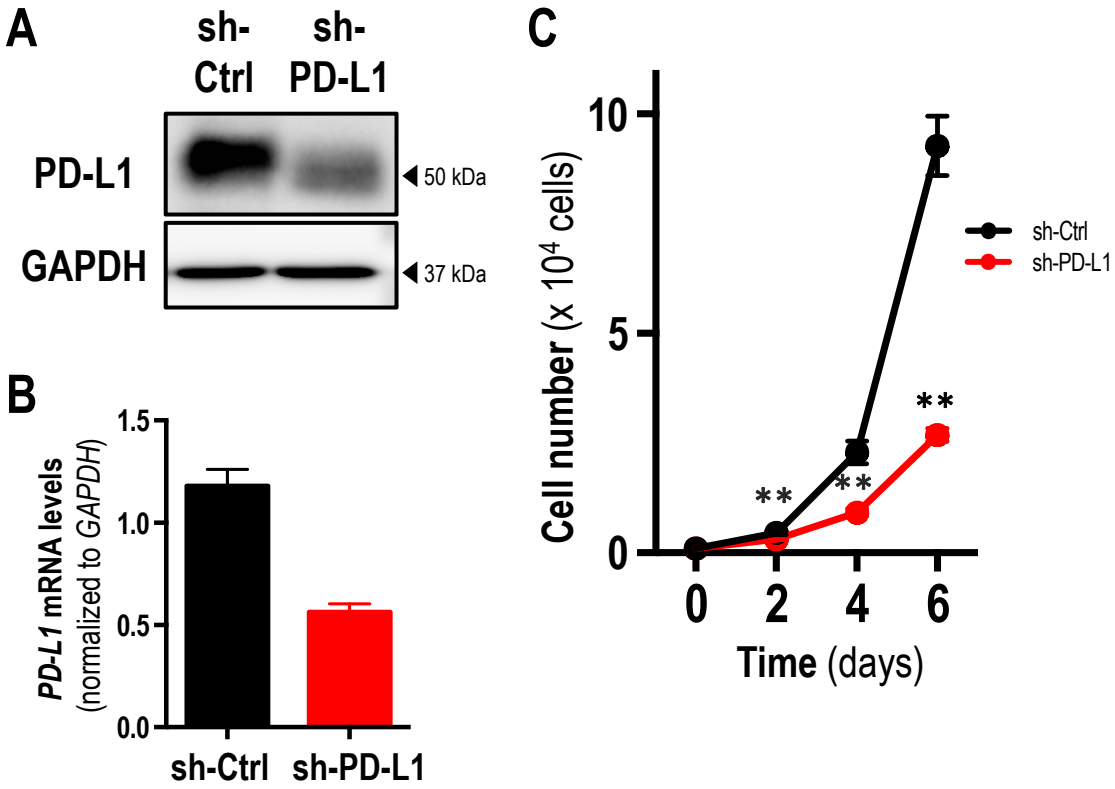
A
sh-Ctrl
sh-PD-L1
PD-L1
GAPDH
50 kDa
37 kDa
B
PD-L1 mRNA levels (normalized to GAPDH)
1.5
1.0
0.5
0.0
sh-Ctrl
sh-PD-L1
C
Cell number (x 10^4 cells)
10
5
0
0
2
4
6
Time (days)
sh-Ctrl
sh-PD-L1
**
**
**

Figure 3

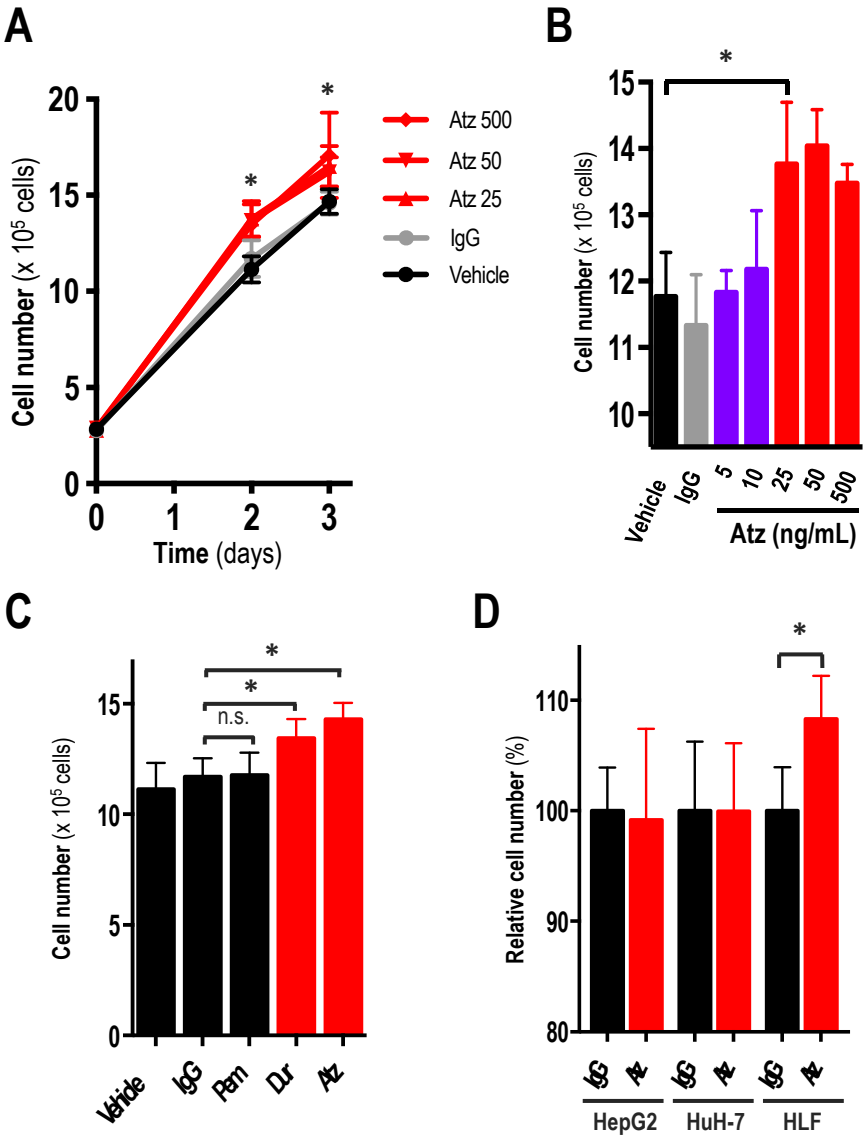
A
Cell number (x 10^5 cells)
Time (days)
Atz 500
Atz 50
Atz 25
IgG
Vehicle
B
Cell number (x 10^5 cells)
Vehicle
IgG
5
10
25
50
500
Atz (ng/mL)
C
Cell number (x 10^5 cells)
n.s.
Vehicle
IgG
Pem
Dox
Atz
D
Relative cell number (%)
IgG
Atz
HepG2
HuH-7
HLF

Figure 4

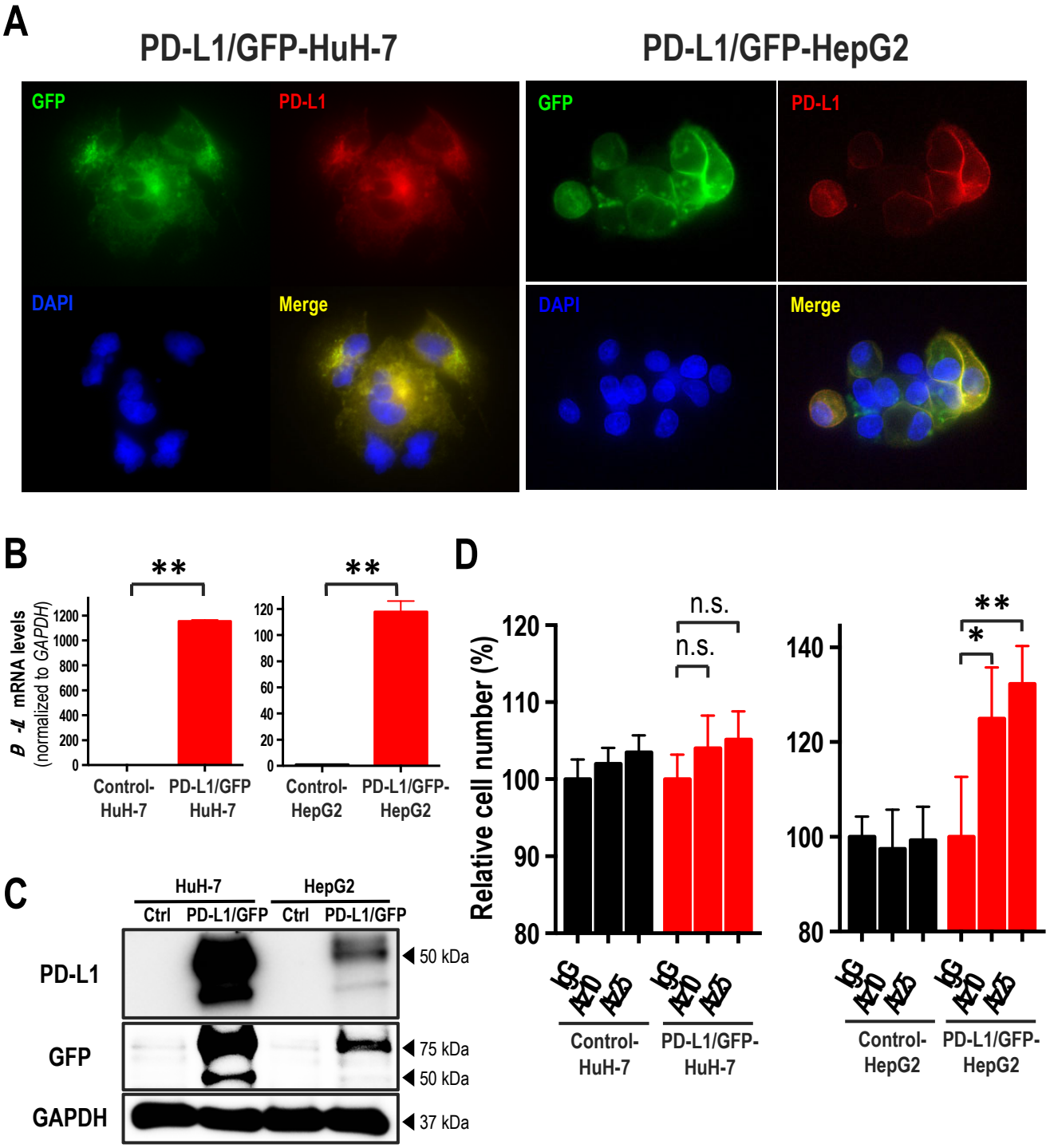
A
PD-L1/GFP-HuH-7
PD-L1/GFP-HepG2
GFP
PD-L1
DAPI
Merge
B
**
**
PD-L1 mRNA levels (normalized to GAPDH)
Control-HuH-7
PD-L1/GFP HuH-7
Control-HepG2
PD-L1/GFP-HepG2
C
HuH-7
HepG2
Ctrl
PD-L1/GFP
Ctrl
PD-L1/GFP
PD-L1
GFP
GAPDH
50 kDa
75 kDa
50 kDa
37 kDa
D
Relative cell number (%)
n.s.
n.s.
**
*
IgG
AZD
MZB
Control-HuH-7
PD-L1/GFP-HuH-7
Control-HepG2
PD-L1/GFP-HepG2

Figure 5

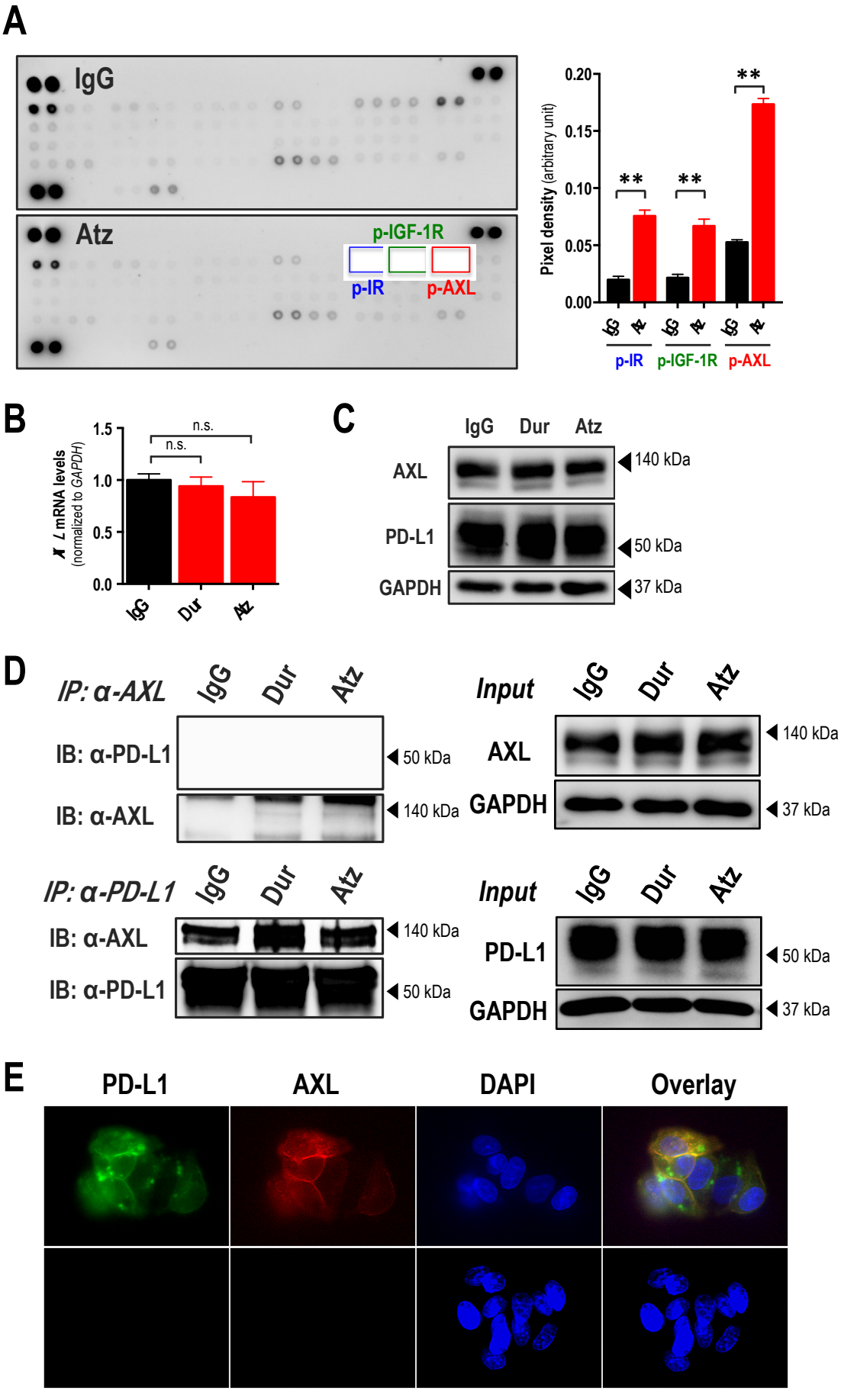
A
IgG
Atz
p-IGF-1R
p-IR
p-AXL
Pixel density (arbitrary unit)
0.20
0.15
0.10
0.05
0.00
**
**
**
IgG
Atz
IgG
Atz
IgG
Atz
p-IR
p-IGF-1R
p-AXL
B
AXL mRNA levels
(normalized to GAPDH)
1.5
1.0
0.5
0.0
n.s.
n.s.
IgG
Dur
Atz
C
IgG
Dur
Atz
AXL
PD-L1
GAPDH
140 kDa
50 kDa
37 kDa
D
IP: α-AXL
IgG
Dur
Atz
IB: α-PD-L1
IB: α-AXL
50 kDa
140 kDa
Input
IgG
Dur
Atz
AXL
GAPDH
140 kDa
37 kDa
IP: α-PD-L1
IgG
Dur
Atz
IB: α-AXL
IB: α-PD-L1
140 kDa
50 kDa
Input
IgG
Dur
Atz
PD-L1
GAPDH
50 kDa
37 kDa
E
PD-L1
AXL
DAPI
Overlay

Figure 5

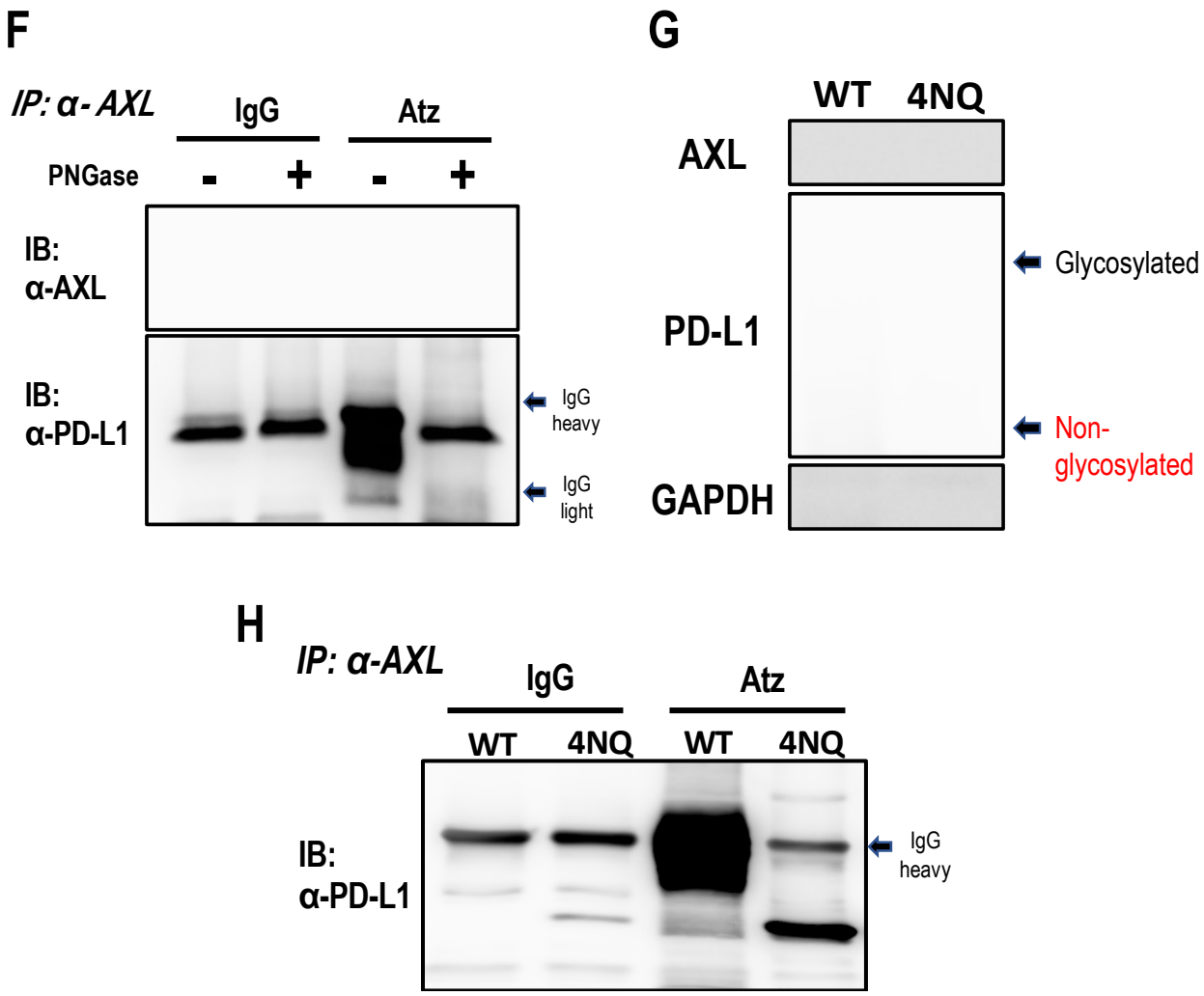
F
IP: α- AXL
IgG
Atz
PNGase
-
+
-
+
IB:
α-AXL
IB:
α-PD-L1
IgG
heavy
IgG
light
G
WT
4NQ
AXL
PD-L1
GAPDH
Glycosylated
Non-
glycosylated
H
IP: α-AXL
IgG
Atz
WT
4NQ
WT
4NQ
IB:
α-PD-L1
IgG
heavy

Figure 6

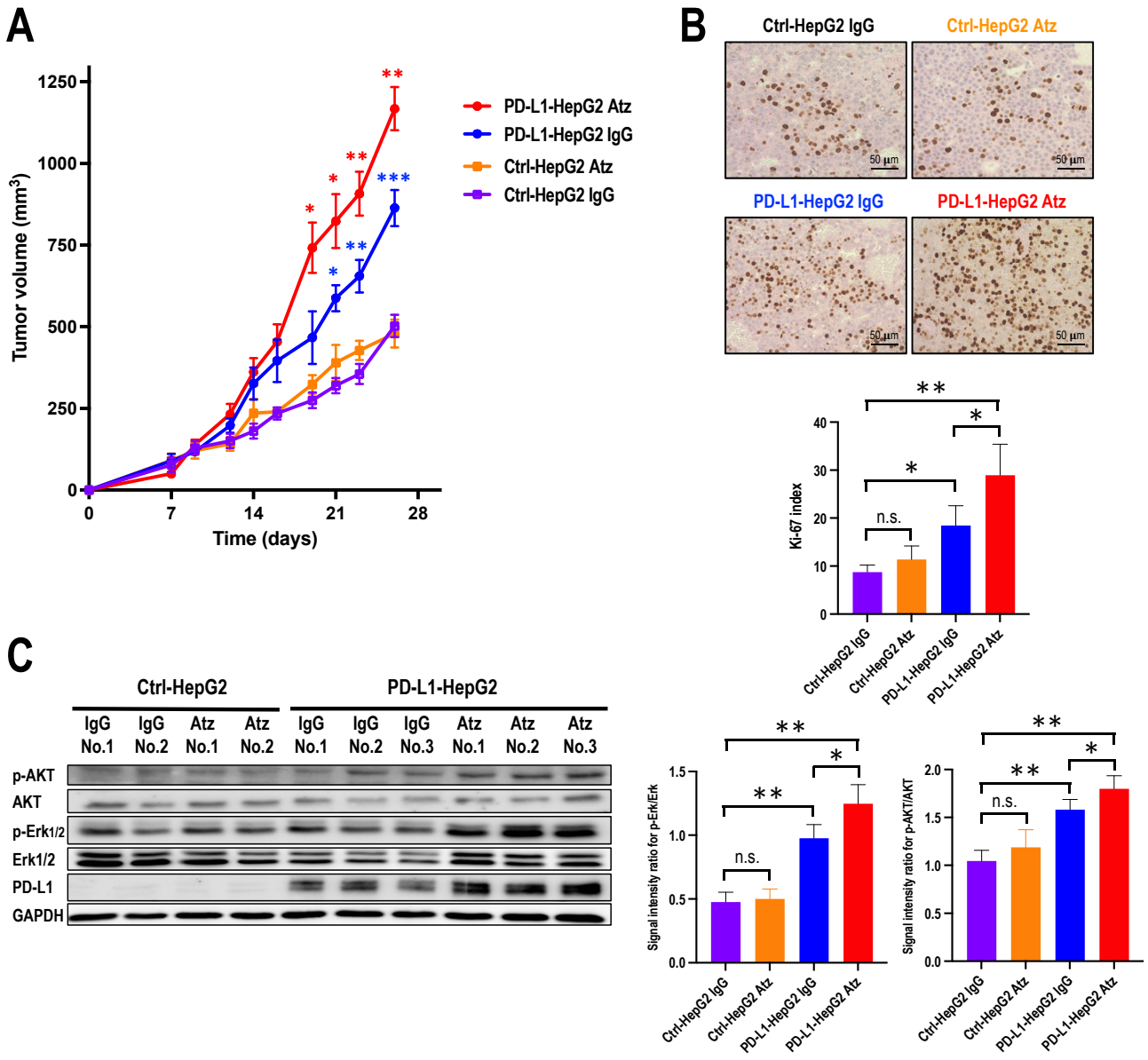
A
Tumor volume (mm3)
Time (days)
PD-L1-HepG2 Atz
PD-L1-HepG2 IgG
Ctrl-HepG2 Atz
Ctrl-HepG2 IgG
B
Ctrl-HepG2 IgG
Ctrl-HepG2 Atz
PD-L1-HepG2 IgG
PD-L1-HepG2 Atz
50 μm
Ki-67 index
n.s.
C
Ctrl-HepG2
PD-L1-HepG2
IgG No.1
IgG No.2
Atz No.1
Atz No.2
IgG No.3
Atz No.3
p-AKT
AKT
p-Erk1/2
Erk1/2
PD-L1
GAPDH
Signal intensity ratio for p-Erk/Erk
Signal intensity ratio for p-AKT/AKT

Table 1. Patients' characteristics

Subjects	All (n=33)
Age (years)	70 [53-79]
Sex	
Female	7 (21%)
Male	26 (79%)
Differentiation grades	
Well	5 (15%)
Moderately	5 (15%)
Poorly	5 (15%)
Sarcomatous	18 (55%)
Previous therapies	
TACE	3 (9%)
None	30 (91%)
Etiology	
Hepatitis B	4 (12%)
Hepatitis C	21 (64%)
Non-viral	8 (24%)
Cirrhosis/Non-cirrhotic	
Cirrhosis	8 (24%)
Non-cirrhotic	25 (76%)

Note: Values are expressed as median [range] or percentage. "Non-viral" include alcoholic liver diseases, non-alcoholic fatty liver diseases, and chronic liver diseases of unknown etiologies.
Abbreviations: TACE, trans-catheter arterial chemoembolization.

Supplementary Figure 1

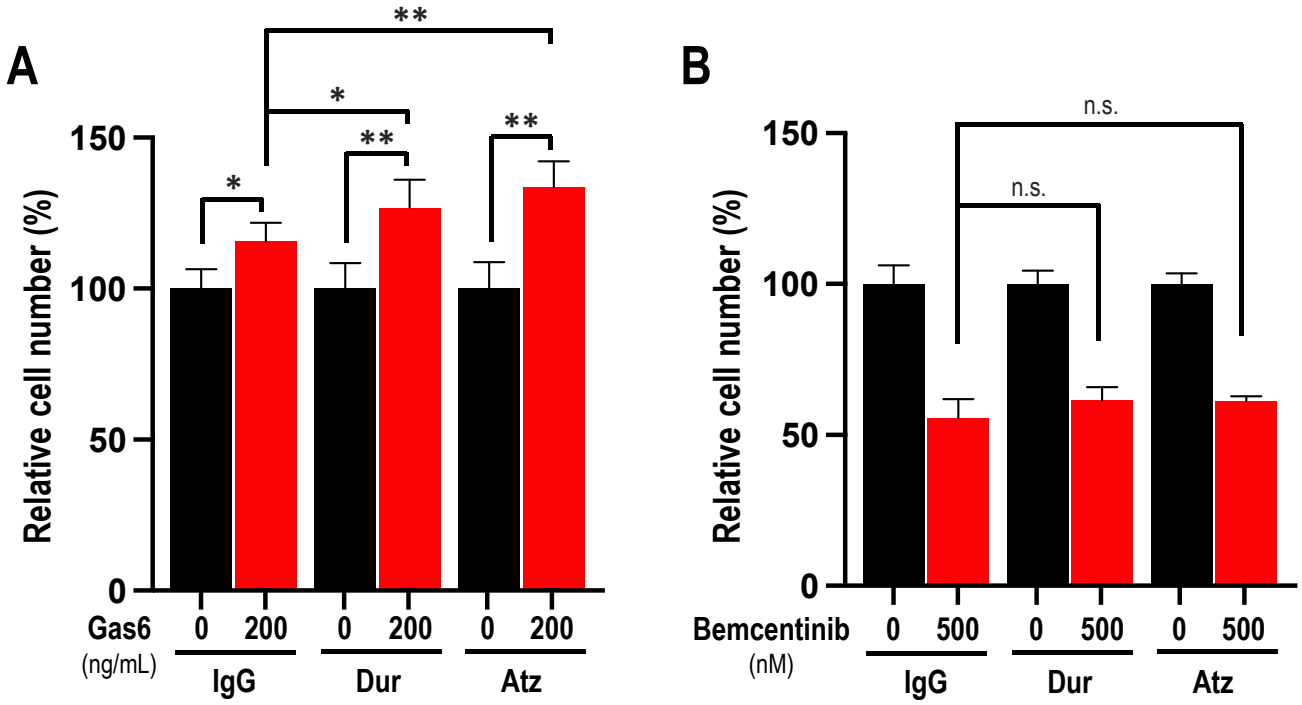

Supplementary Figure 2